DTU

Final report

Novel Humidity Pump using Metal-Organic Frameworks for Indoor Moisture Control

Menghao Qin

June 2023

Novel Humidity Pump using Metal-Organic Frameworks for Indoor Moisture Control

Final report to the Bjarne Saxhof Foundation

2023

DTU, Department of Environmental and Resource Engineering, Bygningstorvet,
Building 115, 2800 Kongens Lyngby Denmark
www.sustain.dtu.dk

Contents

Summary

Latent cooling load accounts for 30% of the total load of air-conditioning, and its proportion is even higher in many tropical and subtropical climates. Traditional moisture control technologies, for example, vapour-compression air-conditioning (VCAC) has a low coefficient of performance (COP) due to the refrigeration dehumidification process, which often makes necessary a great deal of subsequent re-heating. Technologies using conventional desiccants or sorbents for indoor moisture control are even less competitive than VCAC due to their high regeneration temperature, long cycling time and bulky components.

This project has developed a novel humidity pump that uses metal-organic frameworks (MOFs) as desiccant layers, which can efficiently transport moisture from a low-humidity space to a high-humidity one. The working principle and operation modes of the humidity pump were introduced, and the dehumidification performance of the humidity pump was investigated at 22.8℃ with 60% RH. The dehumidification rate and moisture removal efficiency of the MIL-100(Fe) based humidity pump reached to 26.24 g h^{-1} and 0.87 g Wh^{-1}, and these are 2.15 and 2.12 times higher than that of the silica gel-coated one. The humidity pump's maximum dehumidification coefficient of performance (DCOP) could approach up to ~0.46, which is higher than conventional desiccant dehumidification systems. In addition, many factors that may affect the dynamic characteristics and dehumidification performance were analyzed, such as the cycle time, thermoelectric power, and air velocity. Lastly, the localized humidity management ability of the humidity pump using MIL-100(Fe) was validated by a small chamber test. The results indicated that the MOF humidity pump could achieve energy-efficient localized moisture control.

The project was financed by the Bjarne Saxhof Foundation.

1. Background

Energy consumption by buildings has aroused worldwide concern. The building sector accounts for 40% of global energy mainly provided by fossil fuel and corresponds to over one-third of carbon dioxide emissions [1, 2]. The air conditioning system accounts for a significant proportion of the total energy requirement in our living environments. It is worth noting that the latent heat load takes up a large proportion of energy for air handling and particularly for buildings in humid climates [3]. Totally, the latent heat load takes up 20~40% of the air conditioning system [4]. Vapor-compression refrigeration system based on cooling dehumidification is commonly used for indoor temperature and humidity control. During the dehumidification process, the temperature of the air is reduced below the dew point so that the vapor be condensed. However, this dehumidification mode makes the air temperature too low to be directed to the room and needs to be reheated, which caused a waste of energy [5]. The COP of a vapor compression refrigeration system could be increased by about 2.8% and the energy consumption decreased by about 2.5% by raising evaporating temperature 1°C [6, 7]. If the treatment of the latent heat load is decoupled from the sensible cooling, there is no need to reduce the temperature of the evaporator to such a low level. In addition, it is difficult for vapor compression systems to operate with high performance in small space humidity control applications due to its bulk and complex system [8]. Therefore, there is necessary to develop novel moisture control device for localized humidity management with high efficiency.

To remove the latent heat load separately, many efforts have been dedicated to technologies such as solid dehumidification [9, 10], liquid desiccant dehumidification [11, 12], and membrane dehumidification [13, 14]. Combining these dehumidification methods with low-grade energy sources such as solar energy and heat pumps can improve dehumidification and energy efficiency [15-17]. However, the shortcomings and self-limit of these dehumidification methods have not been solved, such as the problem of re-cooling in rotary solid dehumidification, the growth of bacteria in liquid desiccant dehumidification, and so on.

There are also some studies about coating desiccant on the surface of evaporators and condensers to avoid fresh air dehumidification systems and to improve air conditioning efficiency [18, 19]. Chai et al. combined this desiccant-coated heat exchanger (DCHE) with a heat pump for energy saving [20]. Andres et al. investigated the performance of composite silica gel and sodium acetate-coated heat exchangers in the summer and winter seasons [21]. However, the solid desiccant used is silica gel and the high regeneration temperature makes the performance of this device significantly reduced. Cui et al. chose porous metal-organic frameworks (MOFs) as advanced sorbents instead of traditional solid desiccants and the COP of the system was up to 7.9, which demonstrated the superiority of this material [22].

The basic idea of a humidity pump is coming from the analogy of heat pump. A humidity pump is a device that can transport the moisture through an inverse gradient of vapor concentration, which means the vapor can be transferred from a relatively low-humidity space to a high-humidity space. For example, in summer condition, humidity pump will transfer moisture from cool and less-humid indoor condition to a hot and humid outdoor condition; and vice versa in winter condition. Li et al. [8] designed a full-solid-state humidity pump based on silica gel, which exhibited good humidity transfer performance without using refrigerant or cooling water, but the

device is limited to the efficiency of mass transfer and the motor to achieve continuous operation increases the complexity of the device.

Desiccants play an important role in the humidity pump. Traditional desiccants such as silica gel, zeolites possess low adsorption capacity and poor regeneration ability, which limited the development of the adsorption dehumidification system. Though composite desiccant (silica gel-based, carbon-based, et al.) have been prepared by impregnating hygroscopic salt to enhance the adsorption capacity [23], the hygroscopic salts are unstable and easy deliquescence under high humidity. Metal-organic framework (MOF) is a new type of porous crystalline material self-assembled by inorganic metal ions and organic ligands. MOFs possess many good qualities such as huge internal surface area, large micropore volume, physicochemical and chemical variability as well as low regeneration temperature [24, 25]. Although traditional inorganic porous desiccant has been investigated for a humidity pump, the application of MOFs in humidity pump is still worth investigating due to its high potential in moisture transfer.

In this project, a humidity pump based on MOFs has fabricated. The working principle and operation mode of the humidity pump are introduced. The performance and impact factors have been investigated by experiments under different conditions. The localized moisture control ability of the device has been experimentally tested, which provides an important insight to precise moisture control in a confined space.

2. Methodology

2.1 Humidity properties of MOF MIL-100(Fe)

Compared with traditional desiccants, MOFs have great moisture adsorption capacity and transfer rate due to their huge specific surface area and high porosity. However, the MOFs prepared in the early literature had poor water stability, and the pore structure collapsed easily during the process of moisture desorption [26- 29]. MOFs prepared by hydrothermal synthesis reactions generally have better water stability. MIL-100(Fe) is hydrothermally synthesized from metal Fe3+ ions and trimesic acid. MIL-100(Fe) shows great ability to adsorb moisture from the air and can be obtained easily through large-scale synthesis [30-32], which makes it one of the best choices for humidity pump.

The water adsorption characteristics of MIL-100(Fe) were studied in the previous research [21]. Fig. 1 shows the water adsorption isotherms of MIL-100(Fe) at different temperatures. It can be seen that the water adsorption isotherms of MIL-100(Fe) at 20 ℃ has a stepwise increase between 470 Pa (20% RH) and 1170 Pa (50% RH), this S-shape isotherm can make sure cyclical water uptake is close to the maximum adsorption capacity of the dry materials. The difference of moisture content between 20 and 50 °C under 2100 Pa can reach as much as 0.56 kg·kg-1, which means the MOF humidity pump possesses greater potential of adsorption efficiency and has less sensible energy loss for regeneration compared to using traditional desiccant such as silica gel.

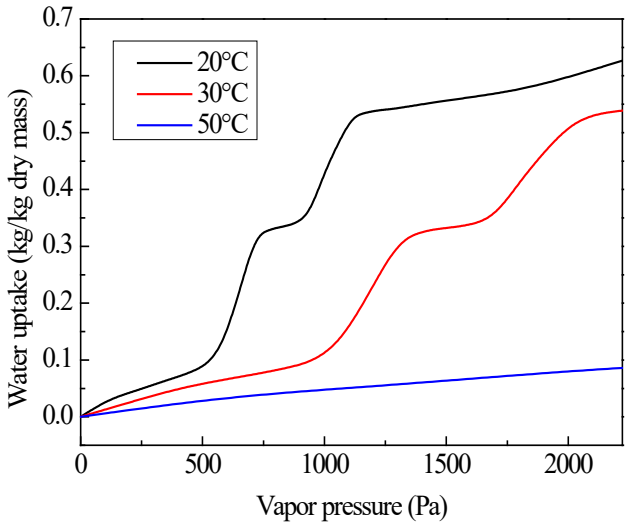

Fig. 1. Water adsorption isotherms of MIL-100(Fe) at different temperatures

2.2 Humidity pump based on MIL-100(Fe)

Fig. 2(a) shows the photo of MOF based humidity pump. The humidity pump device is fabricated by two MOF coated heat exchangers (MOF-HEx), and two thermoelectric coolers. Two aluminum-based plate fins type heat exchangers with the same size (100mm(L)×50mm(W)×60mm(H)) were symmetrically arranged as the heat sinks. The plug-in HEx comprised of 11 fins with a surface area of 0.132 m^2 and 0.5 mm thickness each, and 4 mm width of air channel between each fin. The MIL-100(Fe) was coated on the surface of the fins by a water-borne binder of silica sol, which has no damage to the water sorption characteristics and capacity. The dry mass of the original heat exchangers and coated MIL-100(Fe) was characterized to be 199.6 g and 45.0 g. Two thermoelectric coolers (40mm (L)×40mm (W)×3.8mm (H)) were stuck in the interlayer between the heat sinks by thermal grease to ensure sufficient contact. The remaining part of the heat sinks not covered by the thermoelectric coolers is blocked by silicon sealant to prevent heat transfer between the hot and cold ends.

Bonded heat sinks and thermoelectric coolers were integrated into an enclosed acrylic box (300mm(L)×60mm(W)×130mm(H)) which was divided equally into two-volume with a partition plate. A rectangular cut-out is designed in the middle of the partition plate, corresponding to the size of the surface of the heat sink (100 mm×50mm). The periphery of the heat sinks and the partition plate is coated with hot melt adhesive to ensure airtightness. Both the upper and lower parts of the acrylic box have two 50mm diameter of vents connected to the four-way valves and duct fan through the bellows.

Fig. 2(b) shows the schematic diagram of the MOF based humidity pump. Thermoelectric coolers can absorb and release heat at two opposite sides according to the Peltier effect when the electrical current passes through it. In this way, the adsorption heat during the dehumidification process can be transferred to another side to improve the temperature of the

sink for regeneration. The exchange of dehumidification and regeneration can be achieved through the reverse of electrical current and the switch of four-way valves.

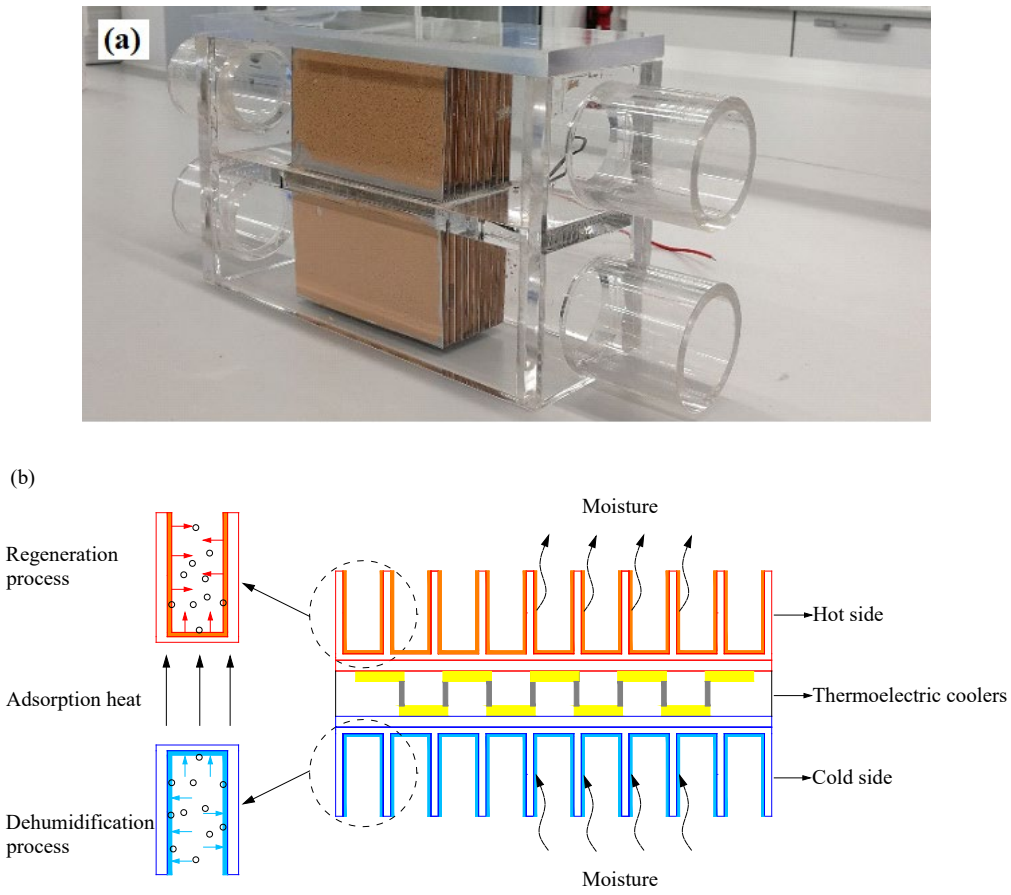

Fig. 2. Photo and schematic diagram of MOF based humidity pump

2.3 Working principle

The dehumidification and regeneration process can be implemented at the same time when the humidity pump starts running. The detailed working principles can be described as the following two parts:

Dehumidification: Typically, there are three ways to achieve dehumidification, which are isothermal dehumidification (O→B1), cooling and dehumidification (O→B2), and isenthalpic dehumidification (O→B3), respectively. The isothermal methods have been considered as the most promising one reported in many refs [8, 22], while other two are not energy-efficient to some extent. In our humidity pump device, the moisture could be adsorbed when the humid air flows through the surface of MIL-100(Fe) coated fins on the cold side, thus the dehumidified air can be obtained with subtle temperature rise (O-B shown in Fig. 3). Based on the thermodynamic analysis, this can be explained by the total heat transferred in the dehumidification side, which consisted of conduction heat and Joule heat from TEC module, convection heat from inlet air, adsorption heat from desiccant and the remaining heat during the

switching. Theoretically, by means of the regulation of input power and ventilation quantity, it is feasible to achieve a quick latent load control through a nearly isothermal dehumidification process, the way close to O→B1 (an ideal path).

Regeneration: As for an ideal regeneration condition, it is preferable to desorb the trapped water vapor in an isothermal regeneration way (O→A1) because this could massively lower the energy consumption. In the actual conditions, the isothermal regeneration is difficult to be achieved, but it is desirable to use less energy source to bring more desorbed water vapor. Considering the interaction between water vapor molecules and desiccant, traditional materials such as zeolite requires high-temperature heat source (>90℃) to go through the regeneration process (O→A2), while MIL-100(Fe) can easily be regeneration with a relatively low-temperature heat source (~50℃) [22]. In this regard, the heat and mass variation of regeneration air in our device should go the way of O→A, which is between O→A2 and O→A1.

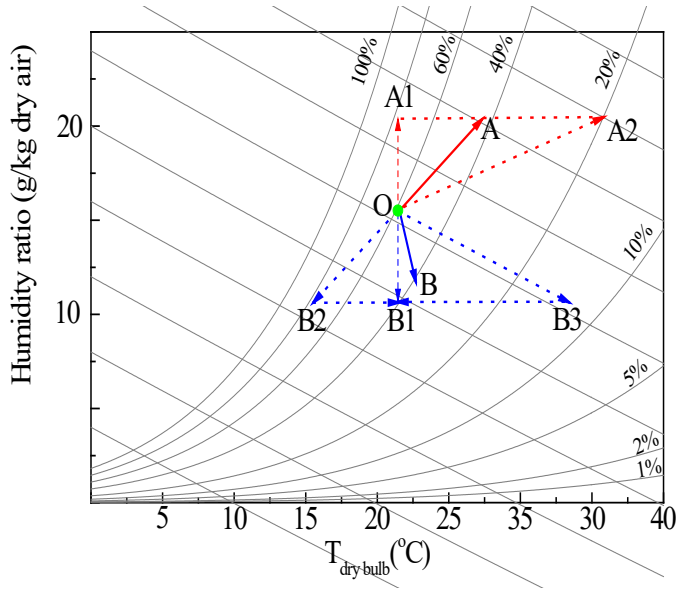

Fig. 3. Working principles: psychrometric chart of the air treating process in our humidity pump.

2.4 Operation modes

In this project, two groups of experiments have been carried out in the aim of: 1) parameter studies (Mode A). 2) Operation performance of localized humidity control for a small chamber (Mode B). The operation parameters including inlet air conditions of dehumidification and regeneration sides are presented in Table 1.

Mode A (Test mode): This mode is designed to conduct the dynamic characteristic and parameter studies. The humidity pump device is placed in a test room (like an air cleaner), the inlet air of both the dehumidification and regeneration sides are the same indoor air. As shown in Fig. 4(a), when the indoor air flows through the dehumidification side, the moisture in the air is adsorbed by the desiccant coated on the fins, leading to the decrease of humidity level. The outlet air from the dehumidification side (dry air) will be supplied to indoor. At the same time,

another group of indoor air enters the device through the inlet for regeneration side and flows through the hot side and takes away the moisture released from the desiccant to dry the MOF coatings. The outlet of the regeneration side will be exhausted to outdoor. When the desiccant in the dehumidification side is saturated, the current flow direction of the thermoelectric cooler is reversed so that the role of dehumidification and regeneration are interchanged. Meanwhile, the only one of four-way valves (outlet) are rotated by 90 degrees and the states are converted from B1 and A1 to B2 and A2, respectively. Such a reciprocating cycle can realize the continuous operation of the MOF humidity pump.

Mode B (Internal recycle mode): This is the intended operation mode for real applications. In this mode, the inlet air of dehumidification side is always the indoor air. The inlet air of the regeneration side is always outdoor air. The outlet air of the dehumidification side (dry air) is supplied to indoor again. The outlet air of the regeneration side (humid air) is exhausted to outdoor. As shown in Fig. 4(b), two four-way valves are used to control the airflow direction. The airflow passages of internal recycle channel and external channel are interchanged. The outdoor air conditions (i.e. temperature and relative humidity) have no impact on the indoor air as the airflow of indoor air and outdoor air is completely separated. The outdoor airflow is only used to take away the heat and moisture released by MOF desiccants during the regeneration process. The MOF humidity pump can also work continually under internal recycle mode through a reciprocating cycle.

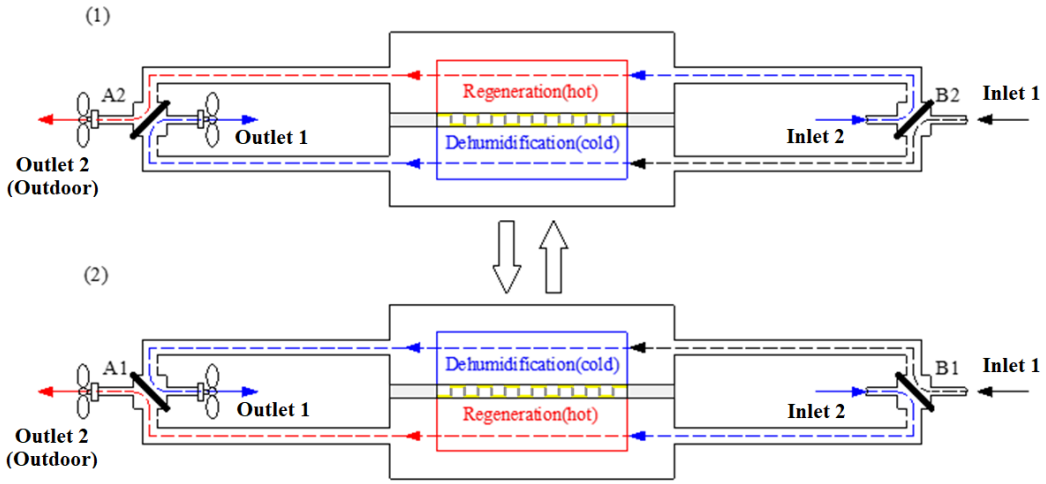

(a) Mode A: Test mode

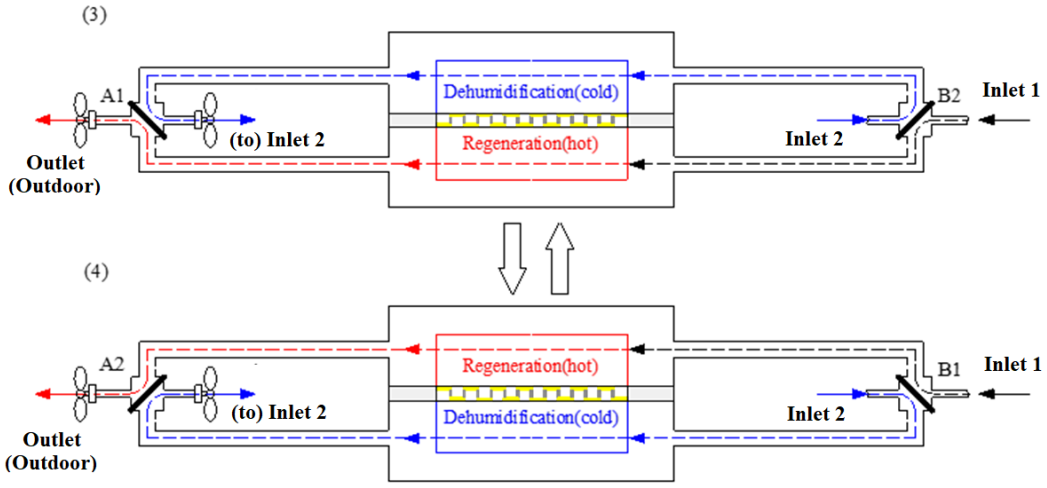

(b) Mode B: Internal recycle mode

Fig. 4. The operation modes of MOF humidity pump:
(a) Test mode, (b) Internal recycle mode

Table 1

Operation conditions of different modes

Operation mode	Parameters	Values
Test mode	Inlet air conditions of De/Re side	22.8℃, 60%RH
	Cycle time	5min, 10min, 15min
	Thermoelectric power	15W, 20W, 25W
	Air velocity	1.5m/s, 3.5m/s, 4.2m/s
Internal recycle mode	Initial inlet air conditions	23℃, 81%RH
	Cycle time	10min
	Thermoelectric power	30W
	Air velocity	2.4m/s

2.5 Experimental measurement

Under working mode, an airflow was conducted to the humidity pump via the duct. The power of the thermoelectric elements was adjusted and recorded. There were no mechanic operations or moving parts in the whole device. Temperature and relative humidity of the inlet and outlet air during the dehumidification and regeneration process were measured by digital hygro sensors with the accuracy of ±0.2 °C and ±2% RH (SEK-SHTC3-Sensors, Sensirion). Airflow rate was adjusted by the variable frequency fan (LH-50P, Jiuyefeng Environmental Technology Co., Ltd.) and recorded by an anemograph (Testo 410-1). The current and voltage of the thermoelectric cooler and the fan under different conditions were recorded for the calculation of the power consumed.

2.6 Performance indexes

To evaluate the performance of the MOF-based humidity pump as the functions of the power input and the temperature and humidity ratio of inlet and outlet air, some parameters herein have been analyzed:

1) The dehumidification rate (E_d) represents the moisture removal over a period of time, which is computed as follows:

$$E_d = \frac{\int_{t_1}^{t_2} q_a(d_{in}-d_{out})dt}{\Delta t} \quad (1)$$

Where E_d (g s^{-1}) is dehumidification rate, q_a (m^3 s^{-1}) is the volume flow. d_{in} and d_{out} (g m^{-3}) are moisture content of inlet and outlet air during dehumidification process, respectively.
2) Moisture removal efficiency (η) represents the power consumption (P_e) to approach to the dehumidification rate (E_d):

$$\eta = \frac{E_d}{P_e} \quad (2)$$

Where P_e (kW) is the total power consumption (including thermoelectric coolers and duct fans).
3) Dehumidification coefficient of performance (DCOP) represents the ratio of air enthalpy variation during the dehumidification process to the total power consumption for the regeneration process:

$$DCOP = \frac{q_a(h_{in}-h_{out})}{P_e} \quad (3)$$

Where h_{in} and h_{out} are the air enthalpy for inlet and outlet process air.

3. Results and discussion

3.1 Dynamic characteristics

The dynamic characteristics of the device are analyzed in terms of inlet and outlet air temperature and humidity. In order to compare the cycling performance of dehumidification and

regeneration side, the same inlet air conditions for these two sides were maintained, thus the detailed experimental conditions were shown as follows: the temperature and relative humidity of the inlet air is about 22.8 °C and 60%. The velocity of the inlet air is 1.5 m s^{-1}. The current of the thermoelectric cooler is 2.66 A, the voltage is 11.32 V, and the calculated power is about 30 W.

Based on the stable conditions, Fig. 5 shows the temperature and humidity variation at the inlet and outlet of dehumidification and regeneration section. Several cycles were performed until stabilization was reached. The operation consists of the dehumidification process and regeneration process. The period from 0 to 10 minutes is the regeneration process corresponding to the regeneration side. The temperature of the outlet air rises sharply at the beginning, and then gradually flattens. The moisture content of the outlet air initially increased in line with the temperature, but then gradually decreased. This is because the vapor in the MIL-100 (Fe) coating is desorbed as the temperature of the heat exchanger rises sharply. As the desorption process proceeds, the water vapor content in the desiccant coating gradually decreases, and the desorption rate also decreases, resulting in a gradual decrease in the moisture content in the outlet air. The dehumidification and regeneration channels were switched over during the period from 10-20min. The outlet air temperature decreased rapidly, but the temperature of the outlet air was still higher than the inlet air. According to the thermodynamic analysis in the previous section, the cooling load of cold side of TEC cannot remove all the sensible loads to be as cool as the inlet air, but the temperature rise was limited. The average outlet temperature at the dehumidification channel was close to 25.5°C. Besides, adsorption heat also increased the air temperature. At the same time, when the air flows through the heat exchanger, the water vapor in the air is adsorbed by the MIL-100 (Fe) coating, and the moisture content decreases sharply. As the coating material gradually becomes saturated from the outside to the inside of the layer, the dehumidification rate gradually decreases.

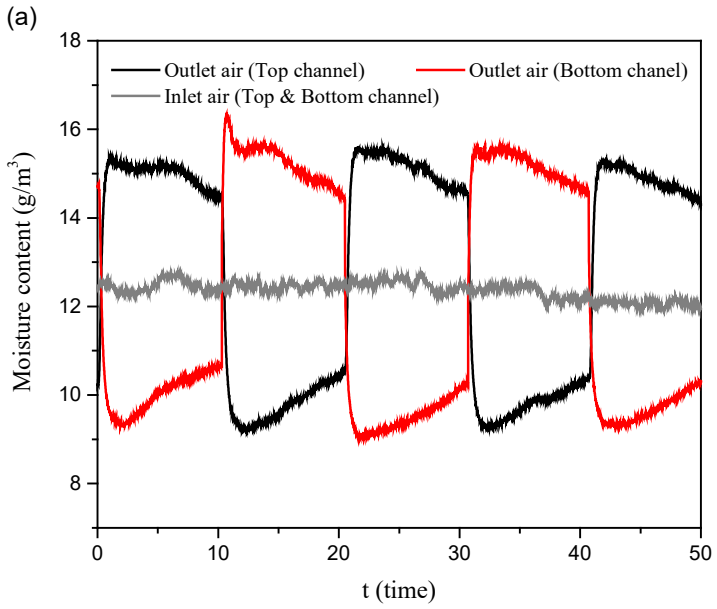

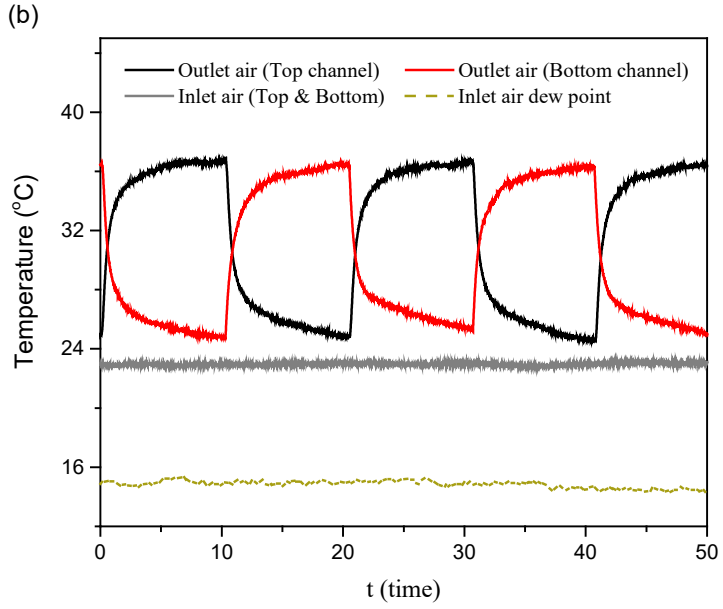

Fig. 5. Temperature and moisture content of inlet and outlet air in Mode A.

3.2 Performance of humidity pump with different desiccants

Fig. 6 shows the difference of moisture content between the inlet and outlet air of the humidity pump with silica gel and MIL-100(Fe) coatings. It can be seen that the humidity pump with MIL-100(Fe) coating shows larger adsorption and desorption rate than that of the silica gel coating, and the attenuation rate is slower. It is because that the regeneration temperature of MIL-100 (Fe) is lower and the moisture storage capacity is larger than that of silica gel. The operation indices are calculated based on Eqs. (1) and (2). The dehumidification rate and moisture removal efficiency of humidity pump with silica gel coating are 12.23 g h^{-1} and 0.41 g Wh^{-1}, and for MIL-100(Fe) coating was 26.24 g h^{-1} and 0.87 g Wh^{-1}, respectively. The values of the MOF based humidity pump were 2.15 and 2.12 times of the silica gel, respectively.

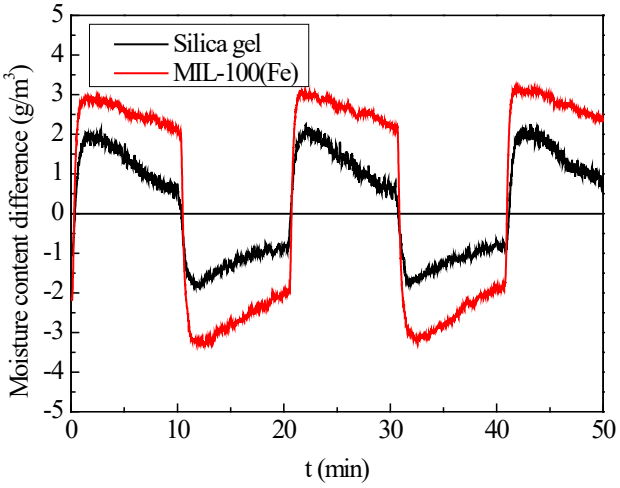

Fig. 6. Moisture content difference of humidity pump using silica gel and MIL-100(Fe).

3.3 Dehumidification performance

3.3.1 Cycle time

According to the previous dynamic characteristics analysis, it can be found that as the operating time goes on, the moisture removed by MIL-100(Fe) coating gradually decreases, which means the cycle time has an important effect on the performances of the device. The power of the thermoelectric power was maintained at 30 W and the air speed was 1.5 m s^{-1}. A series of experiments with different cycle time were carried out and the moisture content difference between inlet and outlet air of the humidity pump was shown in Fig. 7. As the cycle time increased from 5 to 10 and 15min, the peak value of the moisture content difference decreased from -3.10 to -3.35, -3.38 g m^{-3} at the dehumidification side, and increased from 2.92 to 3.18, 3.39 g m-3 at the regeneration side, respectively. The absolute values of the maximum moisture content difference increase with the increase of the cycle time. This is because that the regeneration of desiccant is more sufficient as the cycle time increased. It can also be seen from Fig. 7 that the attenuation of the moisture content difference is more serious with the increase of the cycle time. This is because the desiccant coating gradually becomes saturated with the increase of the operating cycle time and the dehumidification capacity decreases.

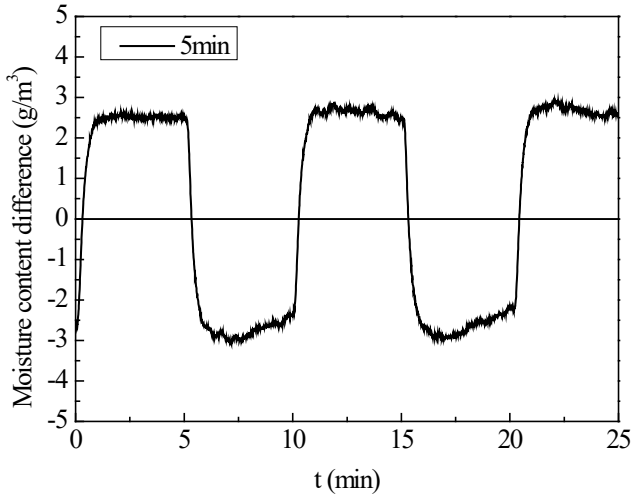

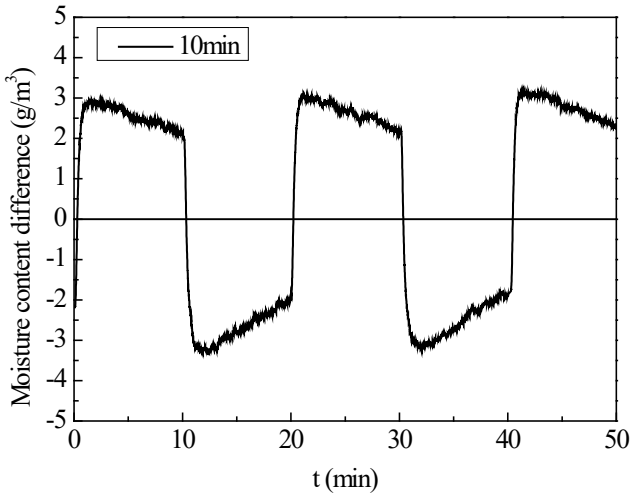

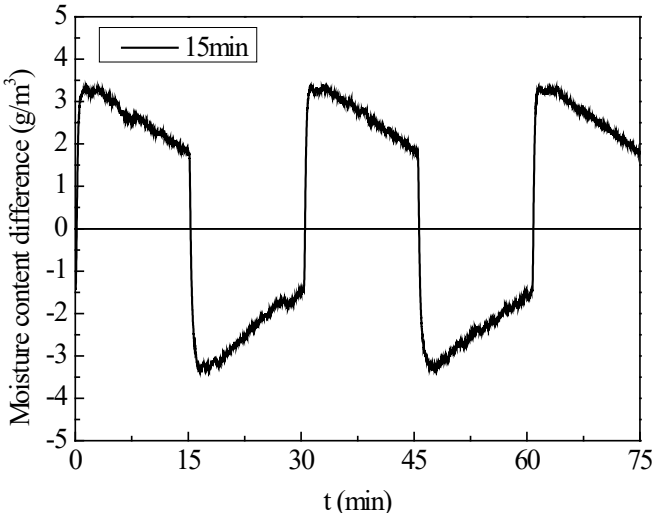

Fig. 7. Moisture content difference of humidity pump with different cycle time

Fig. 8 shows the impact of cycle time on the performance of the humidity pump. The dehumidification rate and moisture removal efficiency increase at first and then decrease with the increase of cycle time. This is determined by the peak value of the moisture content difference and the decay degree, which may be due to the decay characteristics of the adsorption and regeneration ability of the MIL-100(Fe) layers in different cycle time. DCOP increases as the cycle time increases, but the rate of rise was limited after 10min of cycle time in our case.

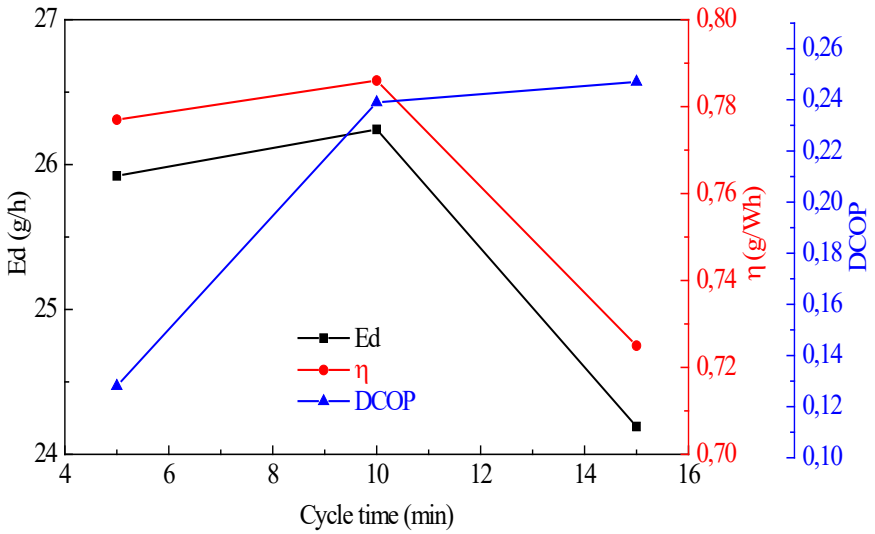

Fig. 8. Impact of cycle time on the performance of humidity pump

3.3.2 Thermoelectric power

Thermoelectric power determined the temperature difference between the hot and cold sides, which has an important effect on the regeneration of the desiccant layer. The cycle time was set to 10 min and the air speed was 1.5 m s-1. Several experiments with different input power of the thermoelectric cooler were carried out and the moisture content difference between the inlet and outlet air of the humidity pump was shown in Fig. 9. Comparing the moisture content difference between the three cases, it can be found that the lower the power, the smaller the moisture content difference between the inlet and outlet air. Particularly for 15 W, there is almost no dehumidification ability at the end of the cycle time. Further analysis found that as the mode changed from dehumidification to the regeneration process, the moisture content difference first rises rapidly and then drops sharply, a tip is formed. The lower the thermoelectric power, the sharper the tip is. Insufficient power results in a lower temperature difference between the hot and cold sides, which affects the regeneration of the desiccant layer.

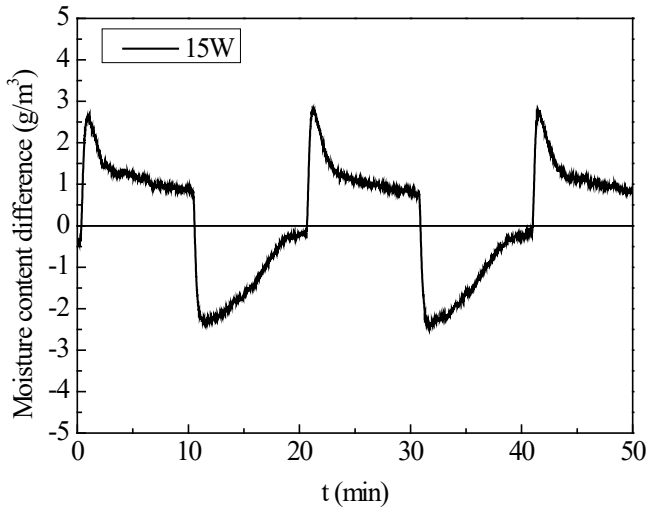

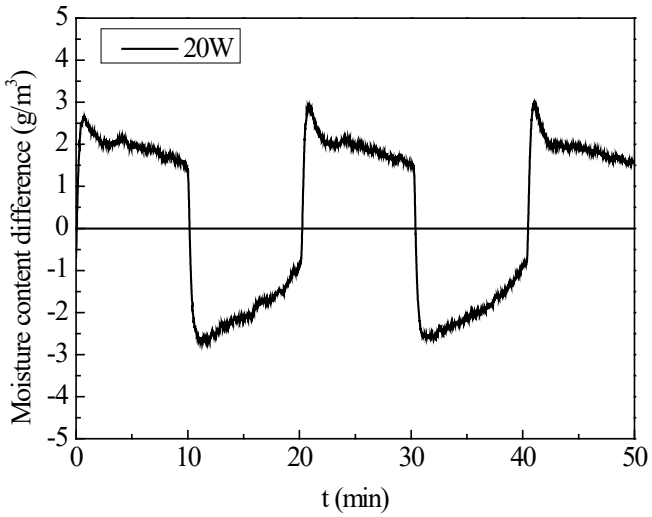

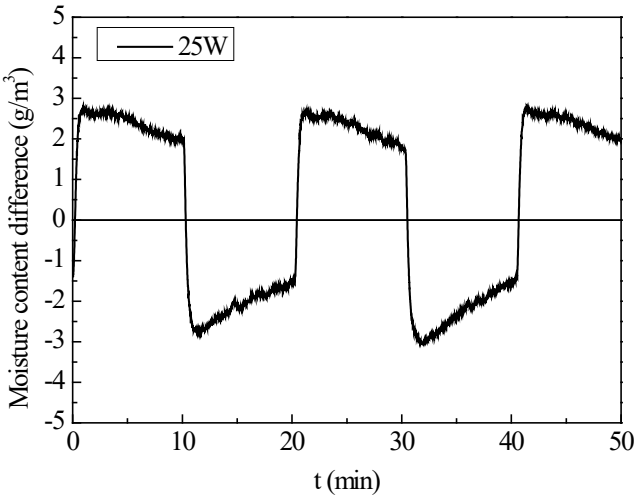

Fig. 9. Moisture content difference of humidity pump with different power

Fig. 10 shows the impact of thermoelectric power on the performance of the humidity pump. The dehumidification rate increases with the increase of thermoelectric power. With the increase of thermoelectric power from 15 W to 25 W, the dehumidification rate increases from 20.5 to 31.9 g h-1. The greater the thermoelectric power, the higher the temperature of the hot side, and the better the regeneration. The moisture removal efficiency increases at first and then decreases with the increase of thermoelectric power, which has the same changing trend as DCOP. In this regard, a too high thermoelectric power would have a negative impact on the moisture removal efficiency and DCOP. As the thermoelectric power is increased to a certain degree, the temperature is enough for the regeneration of MIL-100 (Fe). Excessive power will increase the consumption of energy and has no obvious effect on improving regeneration efficiency.

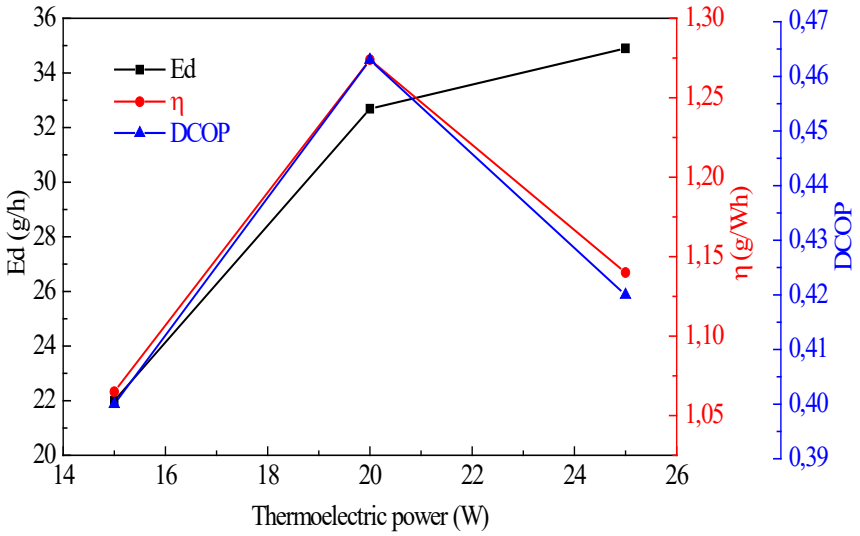

Fig. 10. Impact of thermoelectric power on the performance of humidity pump

3.3.3 Air velocity

Air velocity is another important factor in the characteristics of the humidity pump. The cycle time was set to 10 min and the thermoelectric power was 30 W. Several experiments with variable air velocity were carried out and the moisture content difference between inlet and outlet air of the humidity pump was shown in Fig. 11. The peak value of the moisture content difference between the inlet and outlet air during dehumidification and regeneration processes decreases as the air velocity increases. On the one hand, airflow increases with increasing the air velocity, which would increase the moisture content of the air. On the other hand, heat transfer of the fins was enhanced by increasing the air velocity, which would reduce the temperature of the heat sink and the regeneration performance.

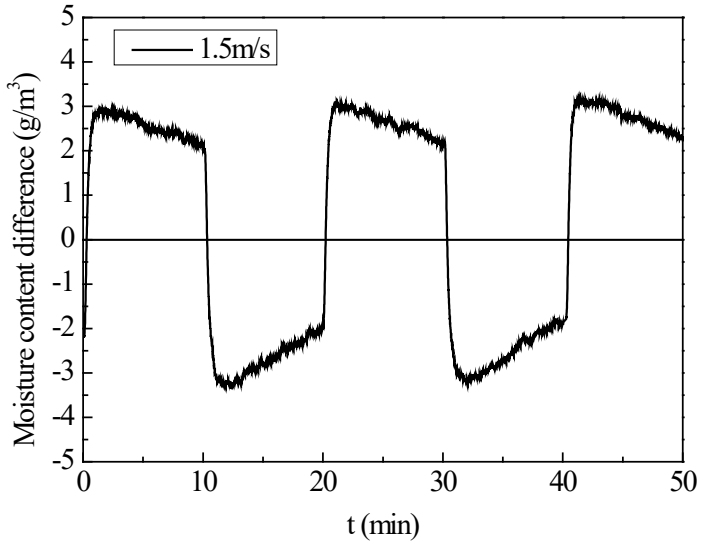

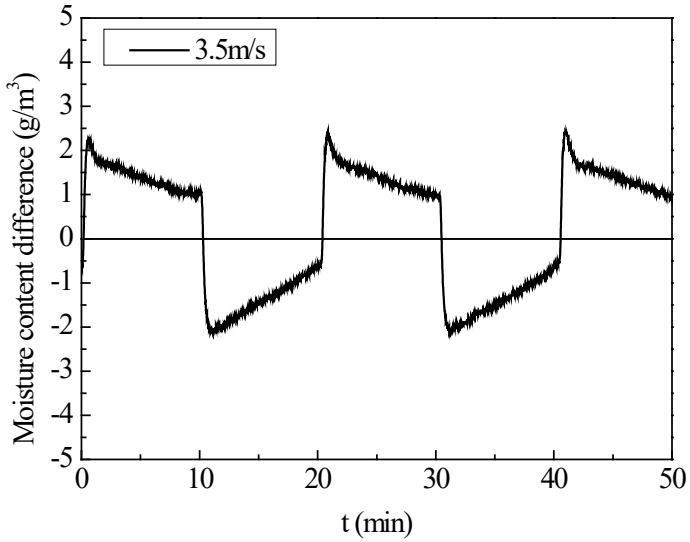

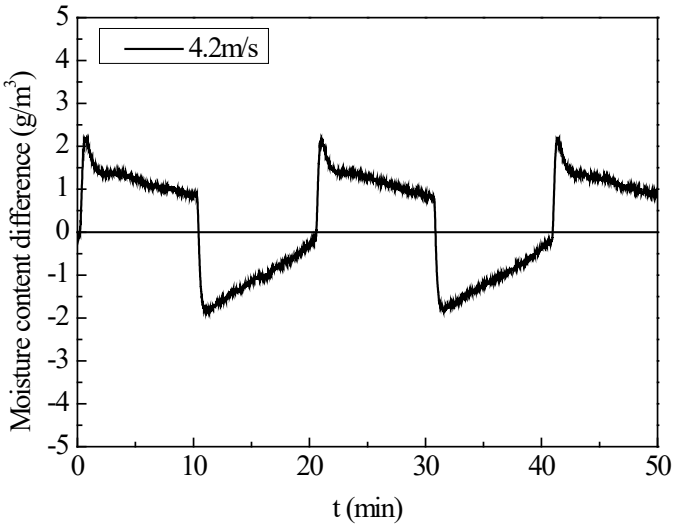

Fig. 11. Moisture content difference of humidity pump with different air velocity

Fig. 12 shows the impact of air velocity on the performance of the humidity pump. Both of the dehumidification rate and moisture removal efficiency increase first and then decrease with the increase of air velocity. Excessive air velocity has a negative effect on the performance of the humidity pump. This is because that the regeneration temperature on the hot sides is reduced as the air velocity increased. Besides, the energy consumption of the pump is also increased with increasing air velocity. However, based on our measured results, it can be found that DCOP can be raised linearly as the air velocity increases. Based on the comprehensive consideration (Ed, η and DCOP), there is an equilibrium point for air velocity around 3.5m/s.

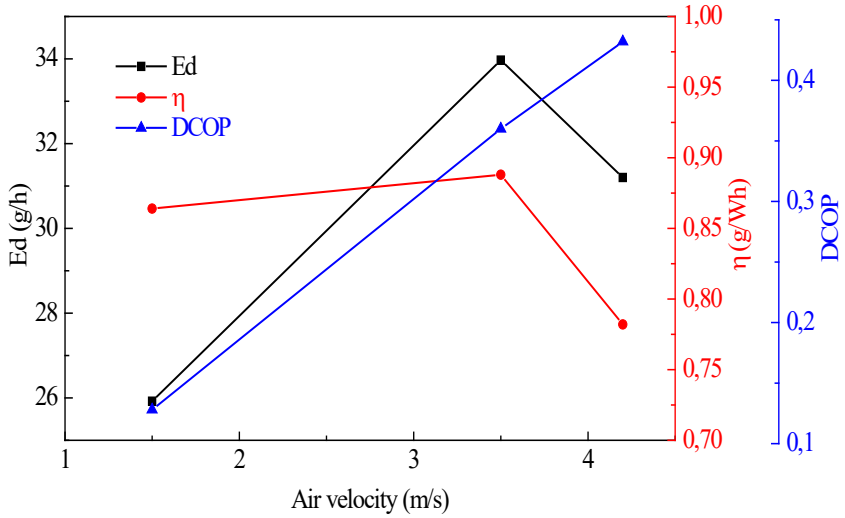

Fig. 12. Impact of air velocity on the performance of the humidity pump

3.4 Humidity control ability

In order to investigate the actual humidity management ability when exposed to a real condition, a test chamber (32.5×54×40.3 cm) made of polystyrene foam (insulation material) was prepared for the humidity pump dehumidification experiment. The initial conditions was maintained at 23 °C and 81% RH (average value), while there are no heat source or moisture dissipation source in the experimental system. The box is connected to the humidity pump through plastic bellows. The schematic diagram of the experimental system is shown in Fig. 13. The operation conditions are shown as follows: the cycle time was set to 10 min, the thermoelectric power was 30W, and the air velocity was 2.4 m s^{-1}. The digital hygro sensors were installed to record the temperature and humidity variation against time.

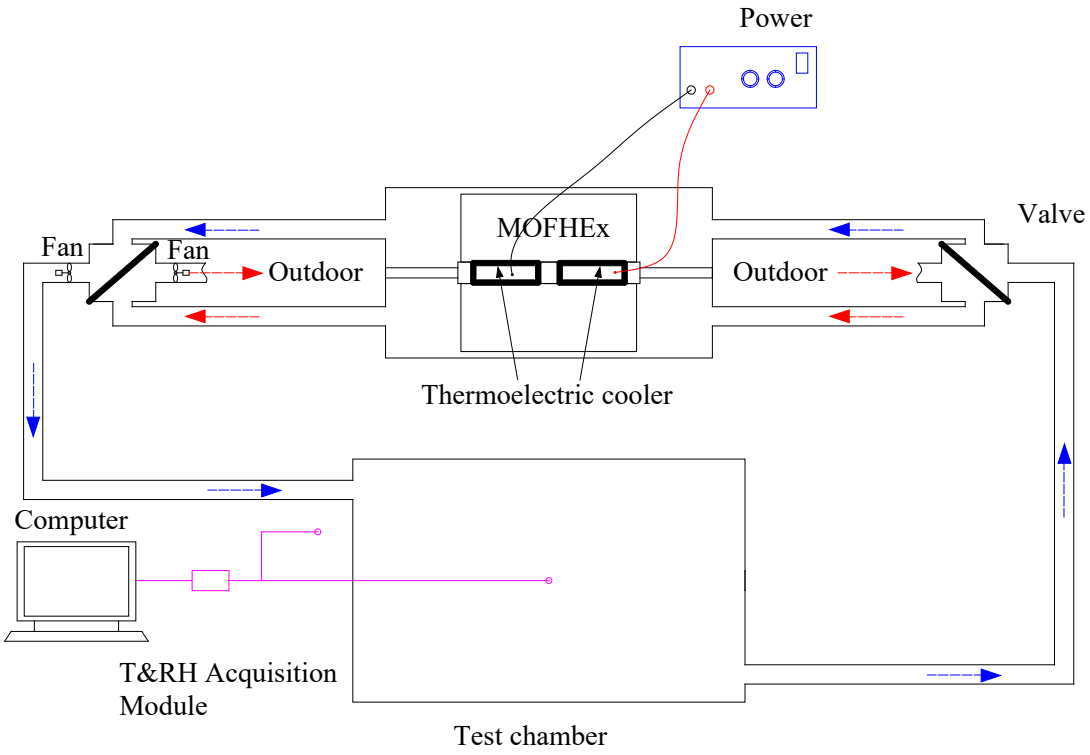

Fig. 13. Schematic diagram of the experimental system

Fig. 14 shows the temperature and humidity conditions inside the test chamber during the experiments. Here the measured results indicate that the temperature on the interior space fluctuates in a zigzag shape. Compared with the environment, the maximum temperature rise of interior space during the experiment is 1.52℃ over 1.3h. This is because the fin temperature cannot be reduced immediately when the regeneration process is converted to the dehumidification process. The relative humidity of the interior space is quickly decreased from ~80% to 38%RH, corresponding to the absolute humidity from 16.7 to 8.2 g m^{-3}. There are there are no heat source and the moisture dissipation sources inside the test chamber. It is important to mention that the interior relative humidity will stop decrease at the trigger point of MOF desiccants, which is around 40% for MIL-100(Fe). It means MIL-100(Fe) will stop adsorb large amount of moisture when the indoor RH is below 40%, which can be clearly seen from the

water sorption isotherm of MIL-100(Fe) [33]. Many MOFs have S-shape isotherms and exhibit a steep uptake isotherm at a specific relative humidity depending on the targeted application [34]. For indoor humidity control, the steep uptake should around 40%. This is one of the main advantages of MOFs over other conventional desiccants. Some MOF materials can autonomously control indoor relative humidity within the desired comfort range at room temperature [35]. Different MOFs have different trigger points and could be used for different moisture control applications [34, 35]. Based on the measurements, it is found that MIL-100(Fe) based humidity pump has satisfactory response to handle the latent load of the test chamber.

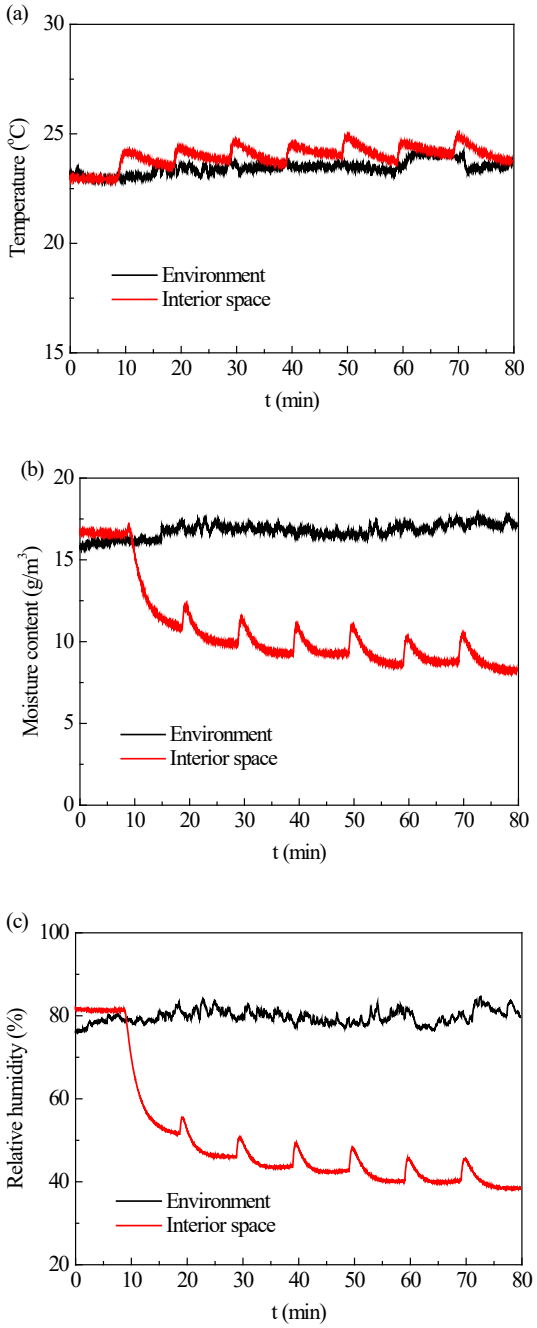

Fig. 14. Temperature and humidity changes inside the test chamber

4. Optimization of the hygrothermal performance

In this section, the optimization of a novel MOF-based humidity pump (MOF-HP) was carried out. We used the CFD method to analyze the hygrothermal performance of a MOF-HP. The model built up the relationship among humid air, desiccant, and heat sink and then coupled the subdomains of the fluid flow, heat transfer, and specie transport. The model of MOF-HP under different operation conditions was validated by experimental tests. Based on the measured results, the discrepancies were maintained under 15%. A parametric optimization was subsequently carried out to enhance the hygrothermal performance of MOF-HP. This dimensional analysis provides some guidelines for MOF-HP design with the most suitable geometry. The optimized configuration is estimated to have a 1.59 times improvement in moisture removal capacity over the original design.

4.1 System analysis

This work aims to investigate the effect of geometrical factors and flow field on the heat and mass transfer to maximize the efficiency of MOF-HP on moisture management. In this case, a 3D model (Fig.15) integrating heat transfer, mass transport, and flow domains was developed to study the geometrical optimization of the MOF-HP. The coating treatment on the fins of the heat sink was adopted in the MOF-HP by referring to other reported configurations [15, 32, 33]. It is noted that the desiccant coating is only considered at the surface of fins in the experiments. The geometry of MOF-HP is shown with details in Table 2.

Table 1 The geometry of MOF-HP.

Parameters	Values
Length of the flow passage, cm	20
Width of the flow passage, cm	6
Height of the flow passage, cm	5
Length of the heat sink (L_x), cm	10
Width of a single channel in the heat sink (W_y), cm	0.495
Height of heat sink (H_z), cm	5
Fin thickness (W_f), cm	0.05
Fin pitch (W_{gap}), cm	0.445
No. of fins (NUM)	11

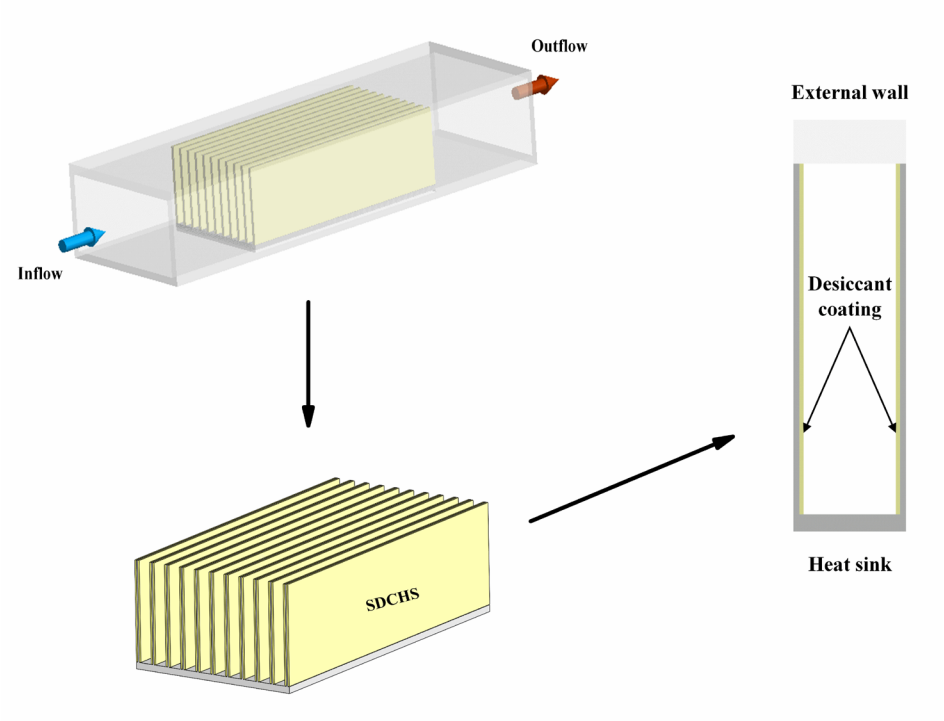

Fig.15. The schematic of MOF-HP.

The fluid in the flow field is humid air, and the solid part of the supporting framework (heat sink) is aluminum alloy. The heat sink was manufactured with specifications shown in Table 2. MOF desiccant- MIL-160(Al) was coated on the surface of fins on the heat sink after the dip-coating process (net weight of coatings: 24.3g). The initial and final mass of the heat sink was measured, and then the thickness was deduced based on the density of desiccant and available coating surface area. The obtained thickness of MOF coatings was compared with the directly measured value using vernier calipers with an accuracy of 0.01mm.

The experiments were designed to measure the cycling performance (i.e., dehumidification and regeneration) of MOF-HP. An air preheater and an ultrasonic humidifier were utilized to control the inlet air states, such as the temperature and humidity. During the dehumidification process, the process air was transmitted by fans to achieve heat and mass transport in the MOF-HP. The desiccant coating removes the extra moisture load, and the heat sink transfers the sensible load. The heat flux from the bottom side of the heat sink can regulate the supply air temperature within a desirable range. When the desiccant coatings approach the saturated state, switching the heat flux from the bottom side of the heat sink can turn the dehumidification mode into regeneration mode. The inlet air with the same conditions passed through the MOF-HP to bring the released moisture away, and this hot and exhaust air was then rejected outdoors. Two digital hygro sensors (SEK-SHTC3-Sensors, Sensirion) were prepared at the inlet and outlet of this device to measure the temperature and relative humidity, which have a 0.5s interval time with an accuracy of ±0.2 °C and ±2% RH. The airflow rate was controlled by a variable frequency fan and measured by an anemograph (Testo 410-1).

4.2 Parametric studies

The proposed modeling of heat and mass transfer has been judiciously validated through experiments in MOF-HP for the complete cycle. Here parametric studies are conducted to comprehensively investigate the effect of geometrical factors and flow field on the MOF-HP's performance. The operation parameters at the following simulations are referred to Case 1, as shown in Table 3.

5.1 (D_r) and DCOP
The performance of MOF-HP is investigated by varying the geometrical size of the unit channel. The horizontal length (Lx) of the heat sink has been increased from 5cm to 14cm, while the height (Hf) and width (Wy) of the unit channel have been changed from 2.5cm to 6cm and1mm to 3.5mm, respectively. These given sizes (Lx, Hf and Wy) defined the exterior framework of a unit channel inside the MOF-HP. The thickness of fin (Wf) and desiccant coating (Wd) are increased from 0.15mm to 0.55mm and 0.15mm to 0.6mm. All the unit channels have been simulated and analyzed with the same inlet air conditions. As for one complete operation cycle, the inlet air is dried during the dehumidification process and humidified during the regeneration process, which is controlled through the switchover of the bottom heat source.

Fig. 16 shows the variation of (D_r) and DCOP in one unit channel when changing the size (Lx, Hf, Wy, Wf, and Wd) of the flow passage. Fig. 8(a) indicates that (D_r) keeps increasing as Lx increases due to the extension of the unit channel (adding more desiccant coating), while DCOP has an evident increase only when γ l⩾0.8. In general, it is preferable to choose a longer Lx for the MOF-HP if there is a size limitation. In Fig. 16(b), it can be found that as the height of the fin increases, there is the maximum (D_r) and DCOP with γf=0.7, and this indicates the trade-off between the heat transfer and mass transport. Similar to that case in Fig. 16(a), the variation of Hf can reflect the total amount of the desiccant coated in the channel and the total surface area of the coating layers. In this regard, though the higher Hf may facilitate the mass transport between the humid air and desiccant coatings, the increased heat resistance may reversely degrade the full adsorption capacity of the coatings. Subsequently, given the same inlet air velocity (~1.1m/s), Fig. 16(c) suggests that the wider size of the unit channel can result in more inlet air (mass flow rate) delivered into the MOF-HP, and then the increased (D_r) and DCOP are found, which means that the increase in the γy can improve the dehumidification of per unit channel. In addition, the thickness of the fin and desiccant coating can directly affect the heat and mass transfer of the unit channel. Fig. 16(d) presents the effect of Wf on the performance of MOF-HP. It is known that the increase in the thickness of the fin can decrease the thermal resistance of the whole heat sink but reversely increase the thermal capacitor (msink·csink). With 0.3-1.1 of γf, (D_r) shows a slight decline from 1.47 g/h/per channel to 1.23 g/h/per channel, and DCOP is decreased from 0.25 to 0.16. As for the thickness of the desiccant coating, Wd, Fig. 8(e) shows that a thicker desiccant coating may improve the (Dr) to a certain degree, but as the thickness increases, (D_r) is decreased. DCOP shows a fast decrease and then maintained around 0.18. According to the results mentioned above, the best unit channel size group (10cm (lx), 5cm (hf), 4mm (Wy), 0.05mm (Wf), and 0.05mm (Wd)) is calculated and shown with 1.99 g/h/per channel and 0.29 of (D_r) and DCOP in Fig. 16(f), which is 1.59 and 1.51 times higher than that of the original Case 1 (γl=γh=γy=γf=γd=1).

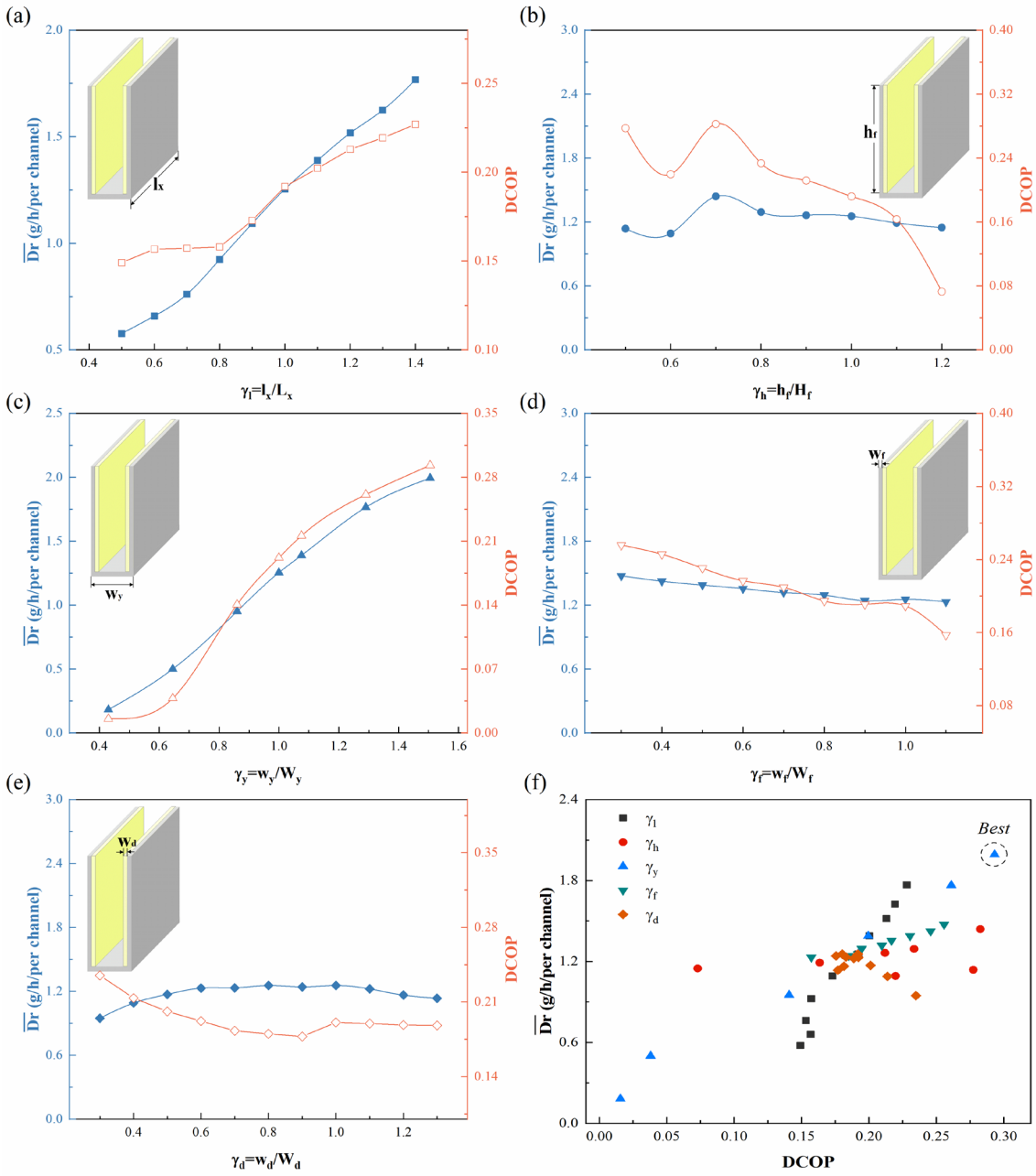

Fig. 16 Effect of geometric sizes on (D_r) and DCOP

4.3 Summary

In this work, the application of solid desiccant coatings on the unit channel of MOF-HP towards the thermal and moisture transport enhancement has been analyzed to provide the optimized geometrical design of the unit channel considering the fluid flow, heat transfer, and moisture transport. The conclusions can be shown as follows:

1) Compared with the conventional air conditioning system, the desiccant-coated humidity pump can regulate the latent load of the surrounding air above the dew point, avoiding the overcooling process.
2) The length (Lx) and width (Wy) of the unit channel can remarkably improve its dehumidification capacity, while the other three sizes (Hf, Wf, and Wd) have a limited effect on the dehumidification capacity. According to the geometry optimization, the best size among the calculated results shows 1.99 g/h/per channel and 0.29 of $\overline{(Dr)}$ and DCOP, 1.59 and 1.51 times higher than that of Case 1
3) The increase in the mass flow rate can affect the dehumidification process at the low mass flow rate range. After a specific value, both $\overline{(D\_r)}$ and DCOP maintained at the constant level.
4) Based on the comprehensive analysis on the flow field and heat transfer, the increase in the sizes (Lx, Hf, Wy, Wf, and Wd) and mass flow rate all can reduce the average thermal resistance, but only the variation in the Hf, Wf, and mass flow rate can lead to the increase in the average Nusselt number. Besides, the thickness of desiccant coatings between 0.5-0.8 of γd may show the best thermodynamic performance.
5) Compared with the bare heat sink, the utilization of desiccant coatings can increase the average surface heat transfer coefficient (related to average bottom temperature) to a certain degree and then be maintained at a constant level. The sensitivity coefficient shows that the desiccant coating can improve the latent load handling, and the recommended thickness of the desiccant is between 0.3-0.5mm.

Since the geometry of the flow channel of a MOF-HP can affect the flow state and thus the heat and mass transfer, the above computational analysis can provide some guidelines to design the optimized geometry of each unit flow channel. Besides, the selection of the desiccant and the integration with different heat sources are also crucial for the full-scale design of the compact solid desiccant humidity pump.

5. Conclusions

In this paper, a novel humidity pump that uses MOF as desiccant layers has been demonstrated. A series of experiments were carried out to investigate the dynamic characteristics and the factors including cycle time, thermoelectric power, and air velocity. The dehumidification rate, moisture removal efficiency and DCOP were also calculated in different conditions. The conclusions are summarized as follows:

(1) The humidity pump can be used to achieve dehumidification above dew point temperature, thereby improving the dehumidification efficiency. Latent heat and adsorption heat can be handled by the desiccant layer and thermoelectric cooler, which can realize the dehumidification and regeneration process at the same time. Four-way valves are used to achieve the continuous operation of the humidity pump and the conversion of the operation mode, which can make the mechanical system simplified.

(2) Dehumidification performance of humidity pumps using MIL-100(Fe) as the desiccant layer is superior to that of silica gel. The dehumidification rate, moisture removal efficiency and DCOP of the MOF based humidity pump can be as high as 34.9 g h-1, 1.14 g Wh-1 and 0.46, respectively, which are all around twice higher than that of silica gel coated systems.

(3) The dehumidification rate and moisture removal efficiency increase at first and then decrease with the increase of cycle time and air velocity, while DCOP increases as temperature rises. The dehumidification rate increases with the increase of thermoelectric power. The moisture removal efficiency and DCOP increase first and then decreases with the increase of thermoelectric power. A too high thermoelectric power would have a negative impact on the moisture removal efficiency and DCOP.

(4) The MOF based humidity pump can achieve a quick localized humidity control. The internal relative humidity level can be maintained at the trigger point of MOF desiccants.

6. References

[1] IEA. Energy Technology Perspectives 2017, ISBN978-92-64-27597-3 (International Energy Agency, 2017)
[2] A. Waqas, Z. Din, Phase change material (PCM) storage for free cooling of buildings-A review, Renew. Sust. Energ. Rev. 18 (2013) 607-625.
[3] L. Harriman, D. Plager, D. Kosar, Dehumidification and cooling loads from ventilation air, 96 (1999) 31-45.
[4] F. Zhang, Y. Yin, X. Zhang, Performance analysis of a novel liquid desiccant evaporative cooling fresh air conditioning system with solution recirculation, Build. Environ. 117 (2017) 218-229.
[5] K. Chua, S. Chou, W. Yang, J. Yan, Achieving better energy-efficient air conditioning–a review of technologies and strategies, Appl. Energy 104 (2013) 87-104.
[6] R. Yumrutaş, M. Kunduz, M. Kanoğlu, Exergy analysis of vapor compression refrigeration systems, Exergy, An International Journal 2 (2002) 266-272.
[7] A. Chan, V. Yeung, Implementing building energy codes in Hong Kong: energy savings, environmental impacts and cost, Energy Build. 37 (2005) 631-642.
[8] B. Li, L. Hua, Y. Tu, R. Wang, A full-solid-state humidity pump for localized humidity control, Joule (2019).
[9] M. Sultan, I. El-Sharkawy, T. Miyazaki, B. Saha, S. Koyama, An overview of solid desiccant dehumidification and air conditioning systems, Renew. Sust. Energ. Rev. 46 (2015) 16-29.
[10] K. Rambhad, P. Walke, D. Tidke, Solid desiccant dehumidification and regeneration methods-A review, Renew. Sust. Energ. Rev. 59 (2016) 73-83.
[11] L. Mei, Y. Dai, A technical review on use of liquid-desiccant dehumidification for air-conditioning application, Renew. Sust. Energ. Rev. 12 (2008) 662-689.
[12] A. Lowenstein, Review of liquid desiccant technology for HVAC applications, HVAC&R Res. 14 (2008) 819-839.
[13] C. Isetti, E. Nannei, A. Magrini, On the application of a membrane air—liquid contactor for air dehumidification, Energy Build. 25 (1997) 185-193.
[14] B. Yang, W. Yuan, F. Gao, B. Guo, A review of membrane-based air dehumidification, Indoor Built Environ. 24 (2015) 11-26.
[15] A. Yadav, V. Bajpai, Experimental comparison of various solid desiccants for regeneration by evacuated solar air collector and air dehumidification, Dry. Technol. 30 (2012) 516-525.
[16] K. Gommed, G. Grossman, Experimental investigation of a liquid desiccant system for solar cooling and dehumidification, Sol. Energy 81 (2007) 131-138.
[17] L. Zhang, N. Zhang, A heat pump driven and hollow fiber membrane-based liquid desiccant air dehumidification system: modeling and experimental validation, Energy 65 (2014) 441-451.
[18] T. Ge, Y. Dai, R. Wang, Z. Peng, Experimental comparison and analysis on silica gel and polymer coated fin-tube heat exchangers, Energy 35 (2010) 2893-2900.
[19] X. Sun, Y. Dai, T. Ge, Y. Zhao, R. Wang, Comparison of performance characteristics of desiccant coated air-water heat exchanger with conventional air-water heat exchanger–Experimental and analytical investigation, Energy 137 (2017) 399-411.
[20] S. Chai, X. Sun, Y. Zhao, Y. Dai, Experimental investigation on a fresh air dehumidification system using heat pump with desiccant coated heat exchanger, Energy 171 (2019) 306-314.

[21] S. Andres, X. Sun, T. Ge, Y. Dai, R. Wang, Experimental investigation on performance of a novel composite desiccant coated heat exchanger in summer and winter seasons, Energy 166 (2019) 506-518.
[22] S. Cui, M. Qin, A. Marandi, V. Steggles, S. Wang, et al. Metal-Organic Frameworks as advanced moisture sorbents for energy-efficient high temperature cooling, Sci. Rep. 8 (2018) 15284.
[23] X. Zheng, T. Ge, R. Wang, Recent progress on desiccant materials for solid desiccant cooling systems, Energy 74 (2014) 280-294.
[24] G. Férey, C. Mellot-Draznieks, C. Serre, F. Millange, J. Dutour, et al. A chromium terephthalate-based solid with unusually large pore volumes and surface area, Science 309 (2005) 2040-2042.
[25] O. Yaghi, M. O'Keeffe, N. Ockwig, H. Chae, M. Eddaoudi, et al. Reticular synthesis and the design of new materials, Nature 423 (2003) 705.
[26] A. Cadiau, Y. Belmabkhout, K. Adil, P. Bhatt, R. Pillai, et al. Hydrolytically stable fluorinated metal-organic frameworks for energy-efficient dehydration Science 356 (2017) 731-735.
[27] D. Alezi, I. Spanopoulos, C. Tsangarakis, A. Shkurenko, K. Adil, et al. Reticular Chemistry at Its Best: Directed Assembly of Hexagonal Building Units into the Awaited Metal-Organic Framework with the Intricate Polybenzene Topology, pbz-MOF [J]. J. Am. Chem. Soc. 138 (2016) 12767-12770.
[28] P. Bhatt, Y. Belmabkhout, A. Cadiau, K. Adil, O. Shekhah, et al. A fine-tuned fluorinated MOF addresses the needs for trace CO2 removal and air capture using physisorption, J. Am. Chem. Soc. 138 (2016) 9301-9307.
[29] J. Low, A. Benin, P. Jakubczak, J. Abrahamian, S. Faheem, et al. Virtual High Throughput Screening Confirmed Experimentally: Porous Coordination Polymer Hydration, J. Am. Chem. Soc. 131 (2009) 15834-15842.
[30] P. Horcajada, S. Surblé, C. Serre, D. Hong, Y. Seo, et al. Synthesis and catalytic properties of MIL-100 (Fe), an iron (III) carboxylate with large pores, Chem. Comm. (2007) 2820-2822.
[31] Y. Seo, J. Yoon, J. Lee, U. Lee, Y. Hwang, et al. Large scale fluorine-free synthesis of hierarchically porous iron (III) trimesate MIL-100 (Fe) with a zeolite MTN topology, 157 Microporous Mesoporous Mater. (2012) 137-145.
[32] P. Hou, M. Qin, S. Cui, K. Zu, Preparation and characterization of metal-organic framework/microencapsulated phase change material composites for indoor hygrothermal control, J. Build. Eng. 31 (2020) 101345.
[33] X. Feng, M. Qin, S. Cui, C. Rode, Metal-Organic Framework MIL-100(Fe) as a Novel Moisture Buffer Material for Energy-Efficient Indoor Humidity Control, Building and Environment, Vol. 145, 2018.
[34] K Zu, M Qin, S Cui, Progress and potential of metal-organic frameworks (MOFs) as novel desiccants for built environment control: A review. Renewable & Sustainable Energy Reviews, Vol, 133, 2020.
[35] M. Qin, P. Hou, Z. Wu, J. Huang, Precise humidity control materials for autonomous regulation of indoor moisture, Building and Environment, Vol. 169, 2020.